Optimisation of device clocking schemes to minimise the effects of radiation damage in charge-coupled devices

Optimisation of device clocking schemes to minimise the effects of radiation damage in Charge Coupled Devices

David J. Hall, Jason Gow, Neil J. Murray, Andrew D. Holland

***Abstract*—The ESA Euclid mission aims to answer the question of how the universe originated through the mapping of the dark Universe. One method to investigate this geometry is to measure subtle changes in ellipticity using image sensors such as the CCD. However, the radiation environment in space plays a major part in the performance of CCD-based camera systems. When placed in space, a CCD becomes damaged by the radiation environment and this can lead to a 'smearing' of the charge, acting to change the ellipticity and therefore one must be able to separate the changes in ellipticity caused by radiation damage from those the mission aims to measure. To this end, the radiation damage induced shape changes require in depth investigation such that optimised operation can be achieved. A Monte Carlo simulation is being used to predict this impact, backed by experimental data from a detector formerly baselined for the mission. During the experimental study, an investigation was undertaken into the serial readout of the CCD to demonstrate an approach towards performance optimisation through a consideration of the trap species involved. A change in clocking scheme was found to result in a factor of three reduction in Charge Transfer Inefficiency.**

***Index Terms*—CCD, CTE, CTI, radiation damage, simulation, trapping**

I. Introduction

This study is based on a CCD designed for the ESA Euclid mission [1] and as such is geared towards the radiation damage expected for this mission. When in orbit, the CCD is subjected to a large number of high energy protons. Displacement damage can be caused by the interactions of these protons with the silicon, causing the development of 'traps' that can capture electrons [2]. This 'radiation damage' induces an increase in Charge Transfer Inefficiency (CTI) to the detriment of the device performance. If the mission objectives require small shape changes to be measured in images, then the 'smearing' of charge due to increased CTI must be understood and reduced as much as possible. If a reduction in CTI can be achieved through easily implemented methods, such as by changing the clocking scheme, then there is the potential for large benefits to the mission.

This work is based on four technical notes composed as part of the Euclid CCD experimental study under ESA funding [3][4][5][6].

II. Charge transfer inefficiency

Charge Transfer Inefficiency (CTI) in CCDs is caused by the removal of signal electrons from a charge packet, followed by their release into subsequent charge packets [7]. The trapping and emission of electrons from charge packets can be modelled using Shockley-Read-Hall (SRH) theory [8][9]. SRH theory models the capture and release of electrons through the use of two exponential time constants. The capture time constant (Equation 1) and emission time constant (Equation 2) relate to the probability of capture and emission respectively through relation with the dwell time, t, as given in Equation 5, where m_e^* is the effective mass of the electron, v_{th} is the thermal velocity, σ is the capture cross-section, n is the electron concentration and x can be replaced with c or e for capture and emission respectively.

$$\tau_c = \frac{1}{\sigma n v_{th}} \tag{1}$$

$$\tau_e = \frac{1}{\sigma N_c v_{th}} \exp\left(\frac{E}{kT}\right) \tag{2}$$

$$N_c = 2\left(\frac{2\pi m_e^* kT}{h^2}\right)^{\frac{3}{2}} \tag{3}$$

$$\frac{1}{2} m_e^* v_{th}^2 = \frac{3}{2} kT \tag{4}$$

$$P_x = 1 - exp\left(\frac{-t}{\tau_x}\right) \tag{5}$$

Using these expressions, the probability of capture and emission of charge in a given time t can be calculated (Equation 5) and therefore incorporated into Monte Carlo or analytical simulations of the charge transfer through the CCD, where t refers to the dwell time under each electrode as detailed in the clock timing diagrams, such as the 'video mode' and 'burst mode' schemes detailed in Section V.

III. Trap species

Several trap species are well known to dominate in CCDs for space missions [7][10], summarised in Table I. Although other trap species have been found experimentally, there is little agreement as to the trapping parameters (energy, cross-section etc) due to the system degeneracy and the difficulty in accurate measurement. For this reason, only the most common and best defined trap species have been considered for the first approximation approach considered here. The variation in trap energy, and hence trap emission time constants (Equation 2), causes varying levels of problems dependent on the clocking

The authors are with the Centre for Electronic Imaging, Planetary Space Sciences Research Institute, The Open University, Milton Keynes, UK (corresponding aurthor email: d.j.hall@open.ac.uk).

scheme of the CCD and the timings involved. Under most circumstances for CCD operation, the capture time constant is short compared to the dwell time and if an electron encounters a trap then capture will occur. The emission time constants in relation to the dwell times under each electrode (t) in the CCD play a major role in determining the impact of electron capture by the various trap species. If $t \gg \tau_e$ then the captured electrons will be released back into the same charge packet many times over during the dwell time. If $\tau_e \gg t$ then the captured electron is effectively lost from the charge packet and the trap will remain filled for many charge transfers. When t and τ_e are similar the process is more complex, as detailed below.

TABLE I
SUMMARY OF TRAP PROPERTIES AS USED IN THIS STUDY, WHERE σ IS THE CAPTURE CROSS-SECTION, N_t^r GIVES AN APPROXIMATE RELATIVE TRAP DENSITY [7] AND τ_e GIVES THE TRAP EMISSION TIME CONSTANT AT -114°C.

Trap	Energy (eV)	σ (cm^2)	N_t^r	τ_e (s)
Si-E	0.46	5×10^{-15}	5	1849
(V-V)$^-$	0.41	5×10^{-16}	1	481
Unknown	0.30	5×10^{-16}	1	156×10^{-3}
(V-V)$^{--}$	0.21	5×10^{-16}	1	220×10^{-6}
Si-A	0.17	1×10^{-14}	10	0.59×10^{-6}

The three main stable defects are shown in Table I and describe the phosphorus-vacancy (Si-E or E-centre) and the oxygen-vacancy (Si-A or A-centre), resulting from impurity atoms in the lattice, and the divancy (J-centre), consisting of two adjacent vacancies: (V-V)$^-$ and (V-V)$^{--}$ [11]. The final trap specified in Table I has been measured experimentally with an energy level of 0.30 eV and is produced from an unknown defect [7].

IV. Capture and emission dynamics

An illustration of the charge capture and release dynamics is shown in Figure 1 for a three-phase CCD, with the spatial direction given horizontally and time shown increasing down the page. Here we use the serial register of the CCD204, similar in design to the commercially available CCD203 [12] and formerly baselined for the Euclid mission, to illustrate the process.

During phase A of Figure 1, the signal electrons sit in the potential wells under the higher voltages (+V). Subject to the appropriate trapping probabilities, on arrival in phase B, the unoccupied trap will capture an electron from the charge packet. As the device clocking continues, the charge packet moves on to phase C. If the trap releases in the dwell time of phase C, then the electron will rejoin the charge packet from which it was captured and there is no net charge loss. If the electron is not released from the trap during phase C then, as shown in the example in phase D, the trapped electron will be released into a following charge packet, resulting in a net charge loss and a 'tail' forming behind the signal (a 'smearing' effect). The time spent in phase C is therefore one of the main deciding factors in determining the probability of net loss.

If the measurement of subtle shape changes is required, such as is the case for the Euclid mission in which the ellipticity is measured, then understanding the effect of radiation damage on the images is essential. If one cannot distinguish between shears caused by gravitational lensing and those caused by the "smearing" effect from radiation damage as described above, then there will be a major impact on the science goals. It is therefore essential that the effects of radiation damage on charge transfer are well understood.

V. Charge transfer

With the strong dependence of the net loss of signal on the timings involved, the clocking scheme can play a major role in determining the impact of the traps on the CTI, particularly with trap emission time constants close to the transfer periods involved. Through the use of two different clocking schemes in the serial register of the CCD204, the scale of this impact can be demonstrated.

As an example, one can consider a three-phase serial register clocking scheme as three pulses (the period in which the clock voltage is high), each with a set pulse duration. To maintain a constant readout rate of 200 kHz, the total pixel-to-pixel transfer time (the pulse period) must remain at 5 µs. Each pulse can therefore be considered with a duty cycle D (where D is defined by the pulse duration as a fraction of the pulse period) between zero and one, equivalent to nanosecond time-scales up to just below 5 µs.

A. Choice of clocking scheme

The video mode scheme, Figure 2, can be considered as a "classic" CCD clocking scheme. Here the second register interval is reduced to increase the reset and signal sampling intervals involved in reading out charge from the device. The burst-mode scheme, Figure 3, maximises the reset and signal sampling intervals but here has both samples taken under the same, elongated clock state to minimise any voltage offsets that may occur because of the feed-through from the other clock pulses. Burst mode clocking is favoured for the dual slope integration approach to CDS, allowing lower read noise performance through a longer sampling time. Whilst the even mode clocking can also be used with the dual slope integration approach to CDS, this introduces a significant DC offset since the clocks are not in the same state when the signal sampling occurs and is affected by a small amount of clock feedthrough on the output node. The balance between read noise and "radiation hardness" must therefore be carefully considered.

In the clock timing diagrams, denoted as sequenced, the potentials applied across the electrodes Rϕ1-3 are shown from low/off to high/on (see Figure 1). The clock pulse ϕR denotes the 'reset' and therefore the start of a single pixel readout. The clock timing diagrams do not show the rise and fall times of a loaded device, whereas the clock pulses 'experienced' by the CCD have an overlap at approximately 50 % of their full amplitude to ensure efficient charge transfer, Figure 4.

B. Video mode clocking

In this example of 'video mode' clocking, the pulses are unevenly spaced. The clocking scheme is shown in Figure 2,

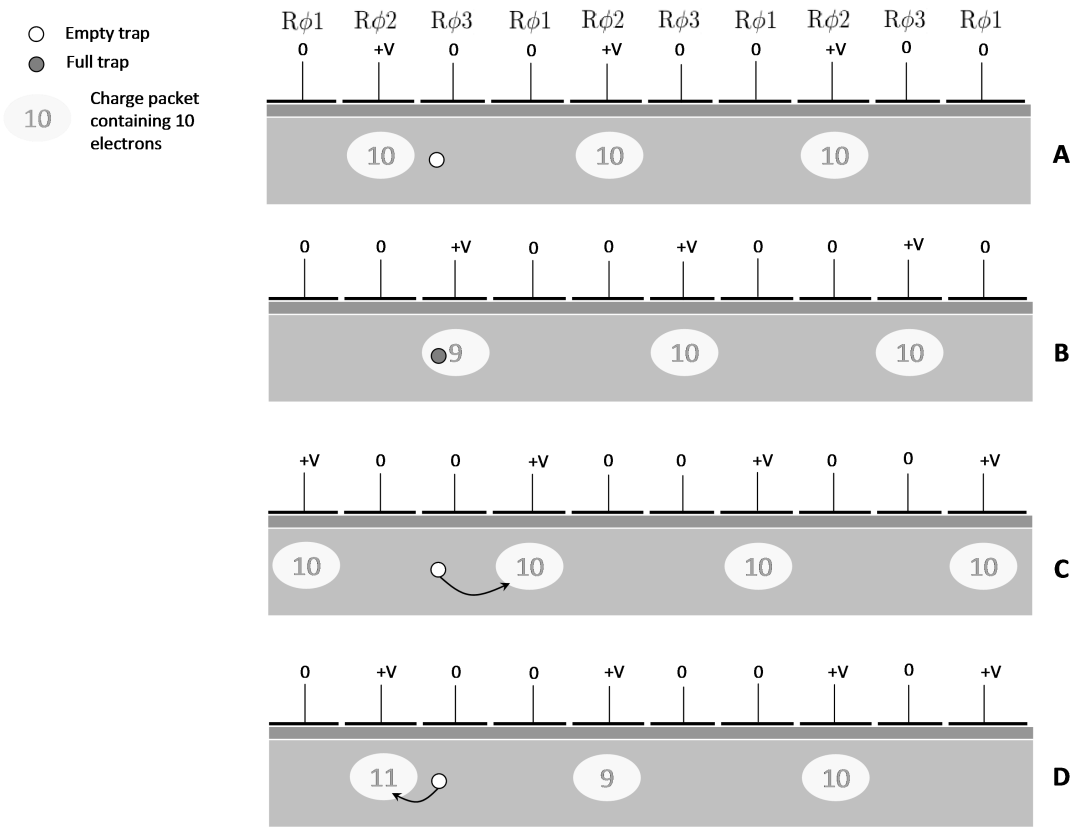

Fig. 1. The capture and release dynamics for charge transfer in a generic three-phase device, shown with the spatial direction horizontally and with time increasing from the top to the bottom of the figure. The charge packet is shown under each of the electrodes as it moves through the device, defining the phases of the clocking scheme that have been examined in this study (Section V); clock overlaps remain constant throughout and are therefore not shown.

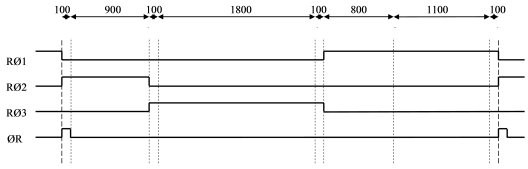

Fig. 2. The 'video mode' clock timing diagram as sequenced, with times shown above the scheme in nanoseconds. Two equal pulses are implemented at 2 µs each followed by a single pulse at 1 µs. [5]

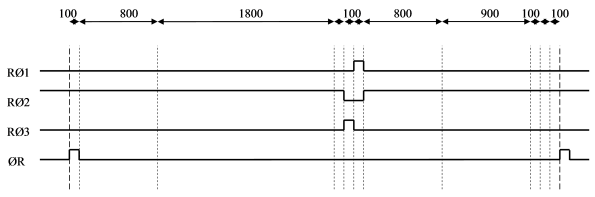

Fig. 3. The 'burst mode' clock timing diagram as sequenced, with times shown above the scheme in nanoseconds. One longer phase dominates in time, followed by two 100 ns pulses. The pixel-to-pixel clocking cycle is 5 µs, the same as that for the 'video mode' scheme shown in Figure 2. [5]

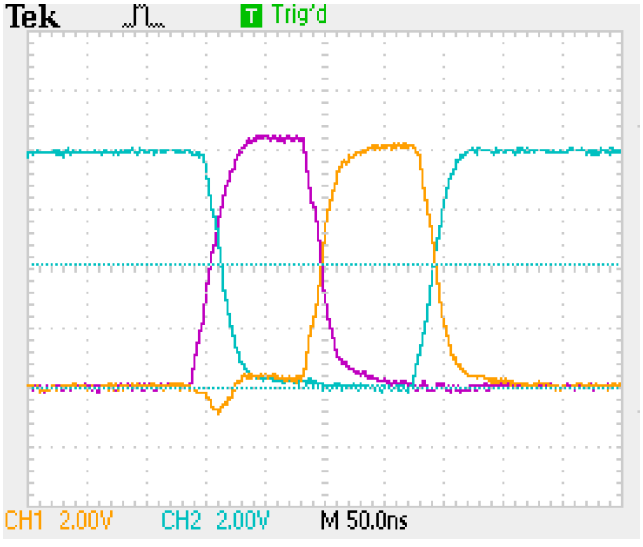

Fig. 4. An oscilloscope output of the burst-mode clock timing sequence as output from the drive system, showing the required overlap at 50% of the full amplitude for efficient charge transfer.

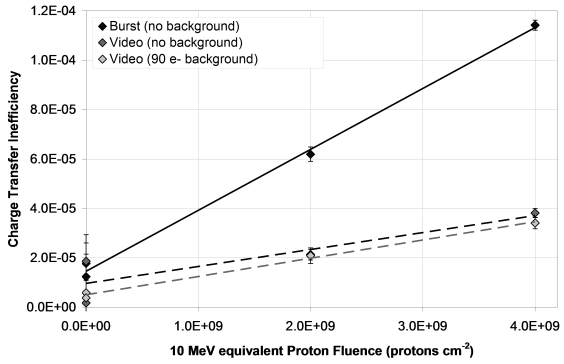

Fig. 5. The serial CTI, measured using Mn-Kα X-rays at a signal level of approximately 1600 e^- as a function of 10 MeV equivalent proton fluence. Results are shown with and without an optical background of approximately 90 e^- [5].

with the first pulse, Rϕ2, lasting for 1 µs (D = 0.2). This shorter pulse is followed by Rϕ3 and Rϕ1, both measuring 2 µs (D = 0.4). The total pixel-to-pixel transfer time is 5 µs, giving a readout rate of 200 kHz.

C. Burst mode clocking

At the alternate extreme, an example of 'burst mode' clocking is shown in Figure 3. In this case, the Rϕ2 pulse lasts for 4.8 µs (D = 0.96), interrupted only by two much shorter pulses of 100 ns each for Rϕ3 and Rϕ1 (D = 0.02). As in the example shown in Figure 2, the readout rate remains at 200 kHz and only the sub-pixel transfers have changed.

VI. CTI Experimental Results

A CCD204 was irradiated in two regions with a 10 MeV equivalent proton fluence of 2×10^9 cm^2 and 4×10^9 cm^2 respectively [5]. For comparative purposes, two regions of the same CCD were left unirradiated. The device was operated at -114°C for the purposes of this study. At this temperature it is thought that the serial register trapping mechanics are strongly dominated by the Si-A. At warmer temperatures for example, Phosphorous Carbon interstitials may begin to interact on the time-scales of the clocking periods (energy of approximately 0.2 eV)[13].

The CTI was measured using the Mn-Kα peak at 5898 eV (approximately 1600 electrons signal), Figure 5, where CTI is defined as the charge lost per transfer per electron present in the initial charge packet pre-transfer.

From these results a clear difference in CTI can be seen between the two clocking modes. The CTI in the serial register for burst mode clocking (Figure 3) is approximately three times higher than that found using the video mode clocking scheme defined in Figure 2.

VII. Monte Carlo Simulation of Charge Transfer in a CCD

In order to match the real-world situation as closely as possible and to offer the best chance of consistency with the experimental data, the Monte Carlo model has been designed over a series of arrays, each with a distinct purpose, including the location of traps in the CCD structure, the trap species and the trap status (filled or empty), amongst other conditions [4]. The electrons forming the 'image' are placed under the second and third electrodes of the CCD during the integration period, as would be found in the real device (at the time of writing). Each trap species is initialised before integration based on the probability of occupation determined from the initial conditions.

The clocking scheme is separated into time slices to reflect each stage inside the pixel-to-pixel cycle and is then programmed directly into the simulation. Each signal charge packet is evaluated under the phases in the CCD as the charge is passed through the arrays, following the clocking timings. The capture and emission analysis is calculated under each and every phase in the CCD before being passed forward by a single phase in the clocking scheme (or spread across a further phase) to ensure the most physical approach to clocking as possible. The parallel and serial modes of the simulation use the appropriate clocking schemes, defined for the two modes from the experimental methods that are being simulated. The serial clocking schemes used in this case are those shown previously in Figures 2 and 3.

The SRH statistics defined previously are implemented for each stage of the charge packet's progression through the CCD. If emission from a trap occurs, the released electrons follow the potential form defined by the clock pulses at the point of release (Figure 1).

A. Charge storage characteristics

Charge capture is a more complex process and therefore requires further explanation. The probability of capture, calculated using the capture time constant τ_c (Equation 1), depends on the electron density at the position of the trap. In the simulation, the traps are located in the volume of silicon such that it is possible for the probability of capture to depend on electron density in three-dimensional space. A Silvaco simulation [14] has been used to model the charge packet volumes in three-dimensions over a range of signal levels. Through a combination of the dwell times at each stage in the clocking scheme and the varying electron density across the charge packet, it is possible to define a 'trapping volume' such that all traps inside the volume (at a specified signal level) will capture and those outside will not. The 'trapping volume' defines the number of traps that will be 'seen' by the signal as it passes through the CCD.

There has been much debate in the literature regarding appropriate approximations that may be used to model the charge storage in the CCD. It has been found that both the proportional model (volume of charge cloud proportional to the signal size) and the fixed charge loss model do not support experimental data, and as such a hybrid of various models has in the past been proposed [7][15][16]. Functions based on Gaussian profiles have been detailed with varying levels of success, but in this case, Silvaco simulations have been used to generate charge storage geometries over a range of signal sizes [17]. Through the use of the charge density profiles simulated

through Silvaco, the Monte Carlo simulation incorporates what is thought to be a much more physical and accurate approach that is not dependent on an approximated Gaussian function [4].

Following the simulation of the parallel transfer, the image is transferred to the serial register. The serial mode simulation is considered in the same way as the parallel mode, with the pixel geometry, signal-volume characteristics and clocking schemes changed to match the serial register properties. The current formulation of the Monte Carlo simulation is costly in terms of the computational time required in comparison to an analytical approach. Further iterations of the simulation code should, through continued study of both the simulated and experimental results, allow the simulation to be operated with greater efficiency [18].

B. Simulating video and burst mode clocking in the serial register

The Monte Carlo simulation has been used to mimic the methods used to produce the experimental data shown previously (Figure 5) at -114°C. The Si-A trap species is considered to dominate in the serial register. Traps with considerably longer emission times can be approximated to remain filled during readout, whilst the $(\text{V-V})^{--}$ can be considered to have negligible impact in comparison to the Si-A due to the factor of 20 reduction in capture cross-section and the reduction in the relative trap density, noting the X-ray flux used in this experimental study of one X-ray event per 80 pixels. The simulation produces serial CTI values in video clocking mode of 3.8×10^{-5} and 3.1×10^{-5} for the low background and 90 electron background respectively. This is consistent within 10 % of the results measured experimentally at 3.8×10^{-5} and 3.4×10^{-5} respectively. The simulated serial CTI for the burst mode operation of 1.20×10^{-4} is consistent with the related experimental CTI of 1.14×10^{-4} .

For both clocking schemes the Monte Carlo simulation is able to reproduce the experimental results to within 10 %. Based on the Monte Carlo algorithms it is therefore possible to consider an analytical approach to better understand the comparative differences in CTI between the two clocking modes.

VIII. Analytical approach

If one considers the trapping with an analytical approach, the variation in CTI can be explained in more detail. To simplify the reasoning, one can consider only the Si-A trap with an emission time constant of 0.59 µs at -114°C. All other traps can be considered to remain filled over the pixel-to-pixel transfer time of 5 µs. The $(\text{V-V})^{--}$ trap with an emission time constant of 220 µs has a capture cross section 20 times lower than that of the Si-A and a trap density approximately ten times lower; the Si-A is therefore considered to dominate over the $(\text{V-V})^{--}$ under these operating conditions.

A. Video mode clocking

Within the microsecond pulses, the capture of charge can be considered to be instantaneous within a volume defined by the signal size and charge density through the Silvaco simulations. Here the emission of electrons from occupied traps is of most importance, with the capture revisited in the following section.

Through a consideration of the probability of emission, it is possible to calculate the net charge loss from a signal packet per pixel-to-pixel transfer: the amount of captured charge which is not released back into the same charge packet from which the capture occurred. There are two cases to consider: capture before the 1 µs pulse (D = 0.2) and capture before a 2 µs pulse (D = 0.4). For charge captured preceding a 1 µs pulse, the probability of emission back into the same charge packet from which capture occurred is 81 % (using Equation 5), resulting in no net charge loss, as in part C of Figure 1. This leaves a probability of 19 % that the charge will be deposited *away* from the charge packet from which it was captured, as in part D of Figure 1, resulting in charge loss and increased CTI. For the case in which charge is captured in the pulse preceding a 2 µs pulse, the probability of no net charge loss is approximately 96 %. Combining the three phases of the video mode clocking scheme, the total pixel-to-pixel charge loss is given by 0.27 times the number of traps seen by the charge packet under one phase for this time-scale.

In summary, if there are N traps that can capture electrons under each of Rϕ1, Rϕ2 and Rϕ3, then $0.19N$ electrons will be lost from under Rϕ1 (preceding the 1 µs pulse of Rϕ2), $0.04N$ from under Rϕ2 and $0.04N$ from under Rϕ3 (both preceding a 2 µs pulse). This gives a total of $0.27N$ electrons lost from the signal packet, where N is the number of electrons captured on the microsecond time-scale under one phase.

Clearly, an increase in the time in which the charge packet sits in the phase adjacent to the one from which it was captured will lead to a lower level of CTI for that step

B. Burst mode clocking

Repeating a similar analysis to that for the video mode clocking, a probability of no net charge loss of 15 % before the 100 ns pulses (D = 0.02) can be calculated (Figure 1, where case C is very quickly passed by). A probability of no net charge loss of nearly 100 % is found before the 4.8 µs pulse (D = 0.96), with case C having a much higher probability than case D due to the timing differences (Figure 1). If the capture probability for each dwell time was constant, the total charge loss from one pixel would be given by 1.7 times the number of traps 'seen' by the signal under one phase. This is, however, not a valid approximation in this case since the number of traps 'seen' by the signal is not equal under each phase; the probability of capture in burst mode clocking cannot be ignored. The capture probability under the 100 ns pulses is considerably lower than that for the 4.8 µs case. The capture is dominated by that under the 4.8 µs pulse, giving a total charge loss of approximately 0.85 times the number of traps 'seen' under one phase (for the appropriate time-scale).

Using the same terminology as above, if there are N traps that can capture electrons under each of Rϕ1, Rϕ2 and Rϕ3 on microsecond time-scales, one should consider only the N traps that can capture electrons under Rϕ2 (due to the 100 ns timings under Rϕ1 and Rϕ3). This gives a total of $0.85N$

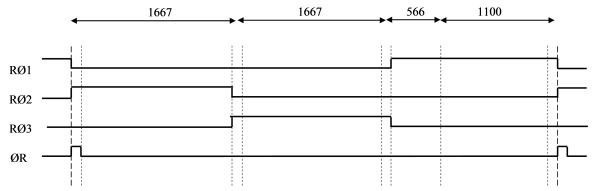

Fig. 6. The proposed optimised clock timing diagram as sequenced, with times shown above the scheme in nanoseconds. Three equal phases provide the minimum net charge loss with a readout rate of 200 kHz. [3]

electrons lost from the signal packet, where N is the number of electrons captured on the microsecond time-scale under one phase.

C. Comparison of clocking schemes

The ratio of charge losses for the burst mode and video mode clocking schemes detailed above indicates that one would, through this analytical approach, expect the burst mode clocking to have 3.1 times the CTI of the video mode, consistent within errors with the experimental and Monte Carlo simulated results detailed previously. Using a similar method, it is possible to minimise the charge loss further still and find the optimum clocking scheme for the serial register under these operating conditions.

IX. Optimisation of the clocking scheme

In order to optimise the serial register clocking scheme, one must consider the advances made through minimising the 'dominant loss pulse' for burst mode clocking, consequently increasing the length of the remaining pulses.

Using this method, one can arrive at the optimal case for this system when each phase is equally spaced. For a 5 µs fixed cycle time, this requires the clocking to be split evenly into three 1.67 µs pulses ($D = \frac{1}{3}$), Figure 6, leaving a probability of no net charge loss of $exp\left(\frac{-1.67}{0.6}\right)$ = 6.2 % per pulse. The total fractional loss is therefore 0.19 times the number of traps 'seen' in each phase by the charge packet over the three phases combined. At this operating temperature, through these approximate calculations, a reduction in the serial CTI of 26 % over the video mode clocking scheme shown in Figure 2 would be expected. Thus, having modified the clocking scheme for the video and burst mode waveforms shown earlier to facilitate signal sampling, at the readout rate and temperatures used here, there may be more to be gained from the improved CTI by reverting to an even mode clocking scheme. However, this may not be the case in all systems and will be dependent on the readout rate and sampling modes used; a careful balance must be considered.

A. Monte Carlo simulation

Using the same Monte Carlo simulation as detailed in Section VII for the video mode clocking, the impact of changing the clocking scheme can be analysed. With no background, the "even clock spacing" scheme (Figure 6) was simulated to have a CTI level 2.8×10^{-5}. The consistency of

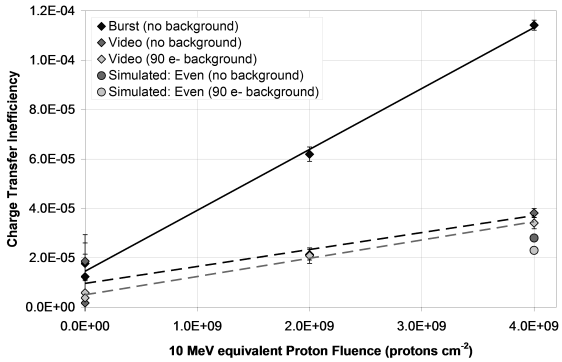

Fig. 7. The experimental data for the two clocking schemes described previously are shown in comparison to the simulated results for the proposed optimised clocking scheme. The CTI has been calculated from a signal of approximately 1600 electrons (Mn-Kα) in both the experimental and simulated results, with both low and 90 e^- background included. With no background, the "even clock spacing" scheme (Figure 6) was simulated to have a CTI level 2.8×10^{-5}, an improvement of approximately 26% [3].

the simulated results with the original burst and video mode clocking schemes improves the confidence in the predicted results. The predicted improvement in CTI of 26% can be seen in Figure 7, simulated for both the low level of optical background and for an increased 90 e^- background.

B. Experimental results

Following the prediction of improved performance through the alteration of the serial register clocking scheme, a further experimental trial was conducted at -113.2±1°C [6] as part of an ESA funded study, Figure 8. Although the results show a slightly lower level of CTI across all clocking schemes, an improvement in serial CTI of approximately 20% is demonstrated. Although this is lower than the 26% predicted by the simulation, the uncertainties in the measured temperature and trap parameters used in the simulation, along with the influence of further trap species in the experimental results is thought to account for the difference. As proposed through the analytical and Monte Carlo simulations, however, the "even clocking scheme" shows clear improvements over the current baseline (at the time of writing).

X. Conclusions

As the requirement for improved performance from detectors for space missions increases, managing the effects of radiation damage will play an ever increasing role in whether science objectives are achievable. Whilst many factors that affect the scope of the radiation damage are controlled by external sources (such as the solar cycle and launch dates, shielding, operating conditions), the clocking of the CCD is one area in which simple changes can produce major improvements in the level of CTI. By keeping a fixed pixel readout rate, the change of clocking timings between electrodes in the readout register of the CCD (moving from 'burst mode' to 'video mode' clocking) can reduce the CTI by up to a factor of 3. Through an understanding of these results and the trapping (capture and emission) involved, one can consider the dominant traps over the clocking time scales

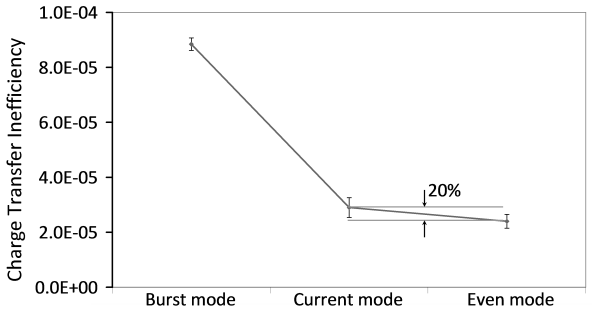

Fig. 8. The experimental data for the three clocking schemes detailed in this study: the current baseline mode (Figure 2), burst mode (Figure 3), and even mode (Figure 6). The experimental data was taken at -113.2±1°C, and therefore shows a slightly lower level of CTI across the board. The proposed "even mode" clocking scheme demonstrates an improvement of approximately 20%.

and therefore predict an optimised clocking scheme. Using a simple analytical approach, backed up through Monte Carlo simulations, it is possible to predict the optimal clocking scheme, as has been shown for the data presented at -113.2°C. For the CCD204 under operating requirements as defined for the current stage of testing for the Euclid mission, this study details an improvement offering a further 20% reduction in the CTI using the "even clocking scheme", allowing an extended mission time before CTI becomes the limiting factor on the science achievable. Preliminary results at -103.2°C and -123.2°C demonstrate that the "even clocking scheme" offers superior CTE performance than both the current baseline and the "burst mode clocking" scheme. However, further investigation is required outside of the current test programme to investigate in more detail the trap species (and their respective parameters) at higher and lower temperatures such that a similar approach can be used to explain the impact of the clocking scheme in more complex cases where the "single dominant trap species" approach is not a valid approximation.

ACKNOWLEDGEMENTS

With thanks to David Burt of e2v technologies for discussion and debate on the subject matter. This study would not have been possible without the work of Gordon Hopkinson and project funding from ESA.

REFERENCES

[1] Cropper M., Refregier A., Guttridge P.,. Boulade O, Amiaux J., Walton D., Thomas P., Rees K., Pool P., Endicott J., Holland A., Gow J., Murray N., Amara A., Lumb D., Duvet L., Cole R., Augueres J.-L. and Hopkinson G., "VIS: the visible imager for Euclid", Proc. SPIE 7731 (2010) 77311J.

[2] Srour J. R., Marshall C.J., and Marshall P.W., "Review of Displacement Damage Effects in Silicon Devices", IEEE Trans. Nucl. Sci., vol. 50, Issue 3 (2003).

[3] Hall D., "Optimisation of the serial register clocking scheme", Open_Euclid_TR_10.01, Technical note, 22nd March 2010.

[4] Hall D., "Euclid Monte Carlo charge transfer simulation", Open_Euclid_TR_09.01, Technical note, 8th April 2010.

[5] Gow J., Murray N. and Holland A., "Optimisation of the serial register clocking scheme", Open_Euclid_TR_07.01, Technical note, 31st March 2010.

[6] Gow J., Murray N., Hall D. and Holland A., "Optimisation of the Serial Register", Open_Euclid_TR_019.00, Technical note, 12th August 2011.

[7] Holland A., "The effect of bulk traps in proton irradiated EEV CCDs", Nuclear Instruments and Methods in Physics Research Section A, 326 1-2 (1993) 335-343.

[8] Shockley W. and Read W. T. Jr., "Statistics of the Recombinations of Holes and Electrons", Physical Review, 87(5), 835-842 (1952).

[9] Hall R. N., "Electron-Hole Recombination in Germanium", Physical Review, 87(5), 387-387 (1952).

[10] Grove A. S., "Physics and Technology of Semiconductor Devices", Wiley (1967).

[11] Gow J., "Radiation Damage Analysis of the Swept Charge Device for the C1XS Instrument", Ph.D. thesis, Brunel University (2009).

[12] e2v CCD203 datasheet, "CCD203-82, Back Illuminated, 4096 x 4096 Pixel Scientific CCD Sensor", A1A-100014 CCD203 Issue 2, Jan 2007.

[13] Private communication, David Burt, e2v technologies.

[14] ATLAS User's Manual, "Device simulation software", SILVACO Inc., 20th April 2010.

[15] Robbins M., "Radiation Damage Effects in Charge Coupled Devices", PhD. Thesis, Brunel University (1992).

[16] Hopkins I. H., Hopkinson G. R. and Johlander B., "Proton-induced charge transfer degradation in CCDs for near-room temperature applications", IEEE Trans. Nucl. Sci., 41 (6) (1994).

[17] Clarke A. S., Hall D. J., Holland A. and Burt D., "Modelling Charge Storage in Euclid CCD Structures", submitted to Journal of Instrumentation, September 2011

[18] Hall D., "Comparison and applicability to the Euclid mission of the ESA CDM and the OU Monte Carlo modelling of CCD radiation damage", Open_Euclid_TR_20, Technical note, 14th April 2010.

BIOGRAPHIES

David Hall David J. Hall was born in the UK in 1984. In 2006 he received an MPhys degree in Physics from Oxford University, UK. He received his Ph.D. degree in the impact of detection physics in X-ray CCD imagers and spectrometers from the Open University in 2010. From 2009 to 2010 he continued as a Research Associate within the *e2v centre for electronic imaging*, part of the Planetary and Space Sciences Research Institute at the Open University in Milton Keynes, UK. His research has included the modelling of charge transfer in CCDs following radiation damage and a study of the impact of radiation damage on spectra for the Radial Velocity Spectrometer forming part the ESA Gaia mission. Since his appointment as an e2v Research Fellow in 2010 he has continued his research within the *e2v centre for electronic imaging* into the modelling of CCDs and novel imaging techniques, with particular interest in the development of innovative techniques and applications for the Electron-Multiplying CCD in synchrotron-based research and medical imaging. Dr. Hall is a member of the Institute of Physics.

Jason Gow Jason received his PhD in 2009 for work on the proton radiation damage effects to the swept charge device (CCD54) used in the Chandrayaan-1 X-ray spectrometer. His work on swept charge devices continued with an initial proton damage study performed using the next generation of devices. These new devices are being studied for possible implementation in the soft X-ray spectrometer on the Chandrayaan-2 lunar Orbiter and the soft X-ray imager on China's HXMT mission. Jason has been involved in the radiation damage assessment of the CCDs for use in the medium class mission Euclid, this has involved an initial assessment of the CCD204 and a comparative study using p-channel CCD47s. He worked with Gordon Hopkinson of SSTL on an ESA funded radiation damage assessment of the CCD204, which combined with discussion between the Euclid consortium and e2v has led to the development of a custom CCD for Euclid, designated the CCD273. Jason is currently working on a like-for-like comparison of p-channel and n-channel CCD204's, previous studies have demonstrated that p-channel CCDs would be well suited for use in hostile radiation environments.

Neil Murray Neil received his PhD degree for work on improvements to MOS CCD technology for future astronomy missions from Brunel University in 2008, where he characterised the X-ray performance of e2vs high-rho sensors that had been developed for near-IR astronomy. In 2008-2010, he followed similar research themes as a Research Associate within the e2v centre for electronic imaging at the Open University (Milton Keynes, UK) developing a soft X-ray camera for an Off-Plane X-ray Grating Spectrometer in collaboration with the UCL-MSSL, University of Iowa, University of Colorado and NASA-Goddard. Currently, the main aspects of his work as an e2v funded PDRA still in the centre for electronic imaging, is to design and build a variety of experiments and techniques to perform detailed characterisation of CCDs in support of the space missions that the group is involved with. Neil also contributes with his technical expertise to the groups wider research interests, as well as those of e2v technologies and provides practical training to groups post-graduate students.

Andrew Holland Andrew is an expert in detector physics and has worked on the development of a number of successful space instruments. Working on a range of detector developments over the past two decades, he has a wealth of knowledge and experience advising on instrument related issues, in particular radiation damage effects and the prediction of orbital performance.